An experimental study on strengthening of vulnerable RC frames with RC wing walls

M. Yasar Kaltakci[a] and Gunnur Yavuz*

*Engineering and Architecture Faculty, Department of Civil Engineering, Selcuk University,
Konya, Turkey*

Abstract. One of the most popular and commonly used strengthening techniques to protect against earthquakes is to infill the holes in reinforced concrete (RC) frames with fully reinforced concrete infills. In some cases, windows and door openings are left inside infill walls for architectural or functional reasons during the strengthening of reinforced concrete-framed buildings. However, the seismic performance of multistory, multibay, reinforced concrete frames that are strengthened by reinforced concrete wing walls is not well known. The main purpose of this study is to investigate the experimental behavior of vulnerable multistory, multibay, reinforced concrete frames that were strengthened by introducing wing walls under a lateral load. For this purpose, three 2-story, 2-bay, 1/3-scale test specimens were constructed and tested under reversed cyclic lateral loading. The total shear wall (including the column and wing walls) length and the location of the bent beam bars were the main parameters of the experimental study. According to the test results, the addition of wing walls to reinforced concrete frames provided significantly higher ultimate lateral load strength and higher initial stiffness than the bare frames did. While the total shear wall length was increased, the lateral load carrying capacity and stiffness increased significantly.

Keywords: seismic strengthening; reinforced concrete (RC); frame; wing wall; reversed cyclic load

1. Introduction

Many buildings in Turkey that were constructed before the introduction of the newer Earthquake Code (TEC 1998) have insufficient strength, ductility or lateral stiffness to resist the effects of an earthquake. The understanding of ductility in TEC 75 and older earthquake codes was not nearly as advanced as that of today's earthquake codes. In addition, the code specifications were not conservative in terms of stiffness and strength. Therefore, buildings designed according to TEC 75 and older earthquake codes are not expected to perform adequately in the event of an earthquake. Outdated earthquake codes are not the only cause of this problem; poor-quality workmanship and weak control mechanisms are also responsible for the production of vulnerable buildings. It is obvious that there will be greater damage to reinforced concrete buildings that were not controlled for quality and were constructed with poor workmanship. The typical characteristics of these

---

*Corresponding author, Assistant Professor, E-mail: gyavuz@selcuk.edu.tr
[a]Professor

buildings are low concrete compression strength, inadequate lateral stiffness, inadequate confinement, lapped splices at the floor levels, strong beam-weak column systems and the usage of plain bars with inadequate development lengths. It is believed that many buildings with these deficiencies would be damaged or even caused to collapse in the event of an earthquake. Therefore, strengthening these buildings is highly important. Different strengthening techniques, such as the addition of infill walls or precast panels, the addition of wing walls, steel bracing systems and the jacketing of columns, are commonly used in practice (Kahn and Hanson 1979, Yamamoto 1993, Sugano and Fujimara 1980, Higashi *et al.* 1984, Fukuyama and Sugano 2000, Yavuz 2005, Jirsa 2006, Yuce *et al.* 2007). The main goal of strengthening is to upgrade or increase the strength, ductility and stiffness of structural members and/or structural systems. In the above-cited studies regarding the addition of infill walls, one-bay, one-story and one-bay, two-story infilled frames were tested under monotonic or cyclic lateral loading. Previous research studies related to partial infill walls were performed in one-bay, one-story and one-bay, two-story reinforced concrete frames (Anil and Altin 2007, Kara and Altin 2006).

One of the most effective and economical methods for the seismic strengthening of existing reinforced concrete frames is the introduction of reinforced concrete shear walls. Test results have shown that infill walls increased the lateral load-carrying capacities of the frames and reduced lateral drift, thereby increasing lateral stiffness. Generally, infill walls are placed between two frame columns by fully infilling the holes of the frames. In some cases, it is not possible for the infill wall to be located fully within the holes of frames because of architectural and constructional restrictions, such as doors or window openings (Fig. 1).

Many types of infill walls and infill reinforcement layouts have been studied in previous research studies (Pincheira 1995, Frosch *et al.* 1996, Canbay *et al.* 2003, Sonuvar *et al.* 2004, Sugano 2006).

Fig. 1 Adding cast-in-place infill walls (from archive of Kaltakci, M.Y.)

In addition, many types of connections from the infill wall to the surrounding frame have been studied, such as shear keys, dowels and chemical anchors (Sugano 1980, Aoyama *et al.* 1984, Frosch 1999).

The main parameters that affect the behavior of infilled frames include the materials and the confinement properties of the infill wall and the surrounding frame, such as the ratio of column flexural reinforcement, the stirrup ratio of the column and the beam, the concrete compression strength, the type of infill material (masonry brick or reinforced concrete), the effectiveness of the connections between the infill and the frame members and the infill reinforcement layouts.

This paper reports an experimental study on the behavior of RC frames with inadequate seismic detailing that were strengthened using RC wing walls under reversed cyclic lateral load reversals. The strength, stiffness, energy dissipation capacities and failure mechanisms of two-story, two-bay RC frames strengthened with cast-in-place RC wing walls were investigated. The main experimental parameters of this study were selected as the ratio of shear wall height to shear wall length and the location of the beam bending bars (inside the shear wall body or not). The test specimens were 1/3-scale, two-story, two-bay RC frames with deficiencies that are commonly observed in Turkey, such as low concrete compression strength, inadequate lateral stiffness, inadequate confinement, lapped splices at the floor levels and the use of plain bars. These frames were first produced as bare frames, and two frames were subsequently strengthened by the addition of RC wing walls with two different lengths. Next, these frames were tested, and the results and theoretical findings are presented and discussed.

2. Experimental study

2.1 Description of test specimens and material properties

In this experimental study, three specimens were produced and tested under reversed cyclic lateral loading. The test frames were 1/3-scale, two-story, two-bay reinforced concrete frames. The frames had deficiencies, including low concrete compression strength, inadequate lateral stiffness, inadequate confinement, lapped splices at floor levels and the use of plain bars. The properties of the test specimens are listed in Table 1. The height and width of the foundation beam were selected as 250 and 330 mm, respectively. The width of the frame members were selected as 85 mm for all of the test specimens.
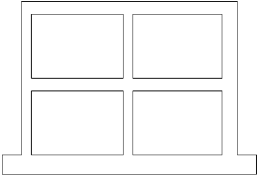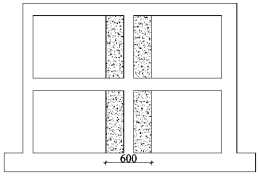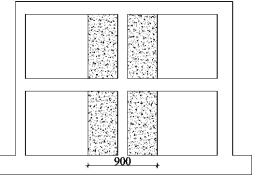
The dimensions and reinforcement details of the specimens are shown in Fig. 2. The dimensions and reinforcement layouts of the frame members (columns and beams) for all of the frames are shown in Table 2.

In the columns, plain bars with a diameter of 8 mm were used as longitudinal reinforcements, and plain bars with a diameter of 4 mm spaced at 100 mm were used as closed stirrups with 90° hooks through the column height. Three plain bars with a diameter of 6 mm were used as longitudinal reinforcements in the beams. Plain bars with a diameter of 4 mm spaced at 100 mm were used as closed stirrups with 90° hooks in the beams through the beam span.

The reinforcement layouts, the dimensions of the wing walls and the dowel spacing with the embedment lengths of the anchorage bars used in the strengthening of the frames are shown in Fig. 3 and Fig. 4. These reinforcement details were determined according to TEC 2007.

Connections between the frame and the wing walls were achieved by using anchorage dowels,

Table 1 Properties of test specimens

Specimen no		BF	SWF600	SWF900
Shear wall configuration				
Lw (mm)		-	600	900
Hw (mm)		-	2000	2000
Hw/Lw		-	3.33	2.22
fc (MPa)	Frame	14	14	14
fc (MPa)	Shear wall	-	30	30

Lw: total shear wall length, Hw: total shear wall height
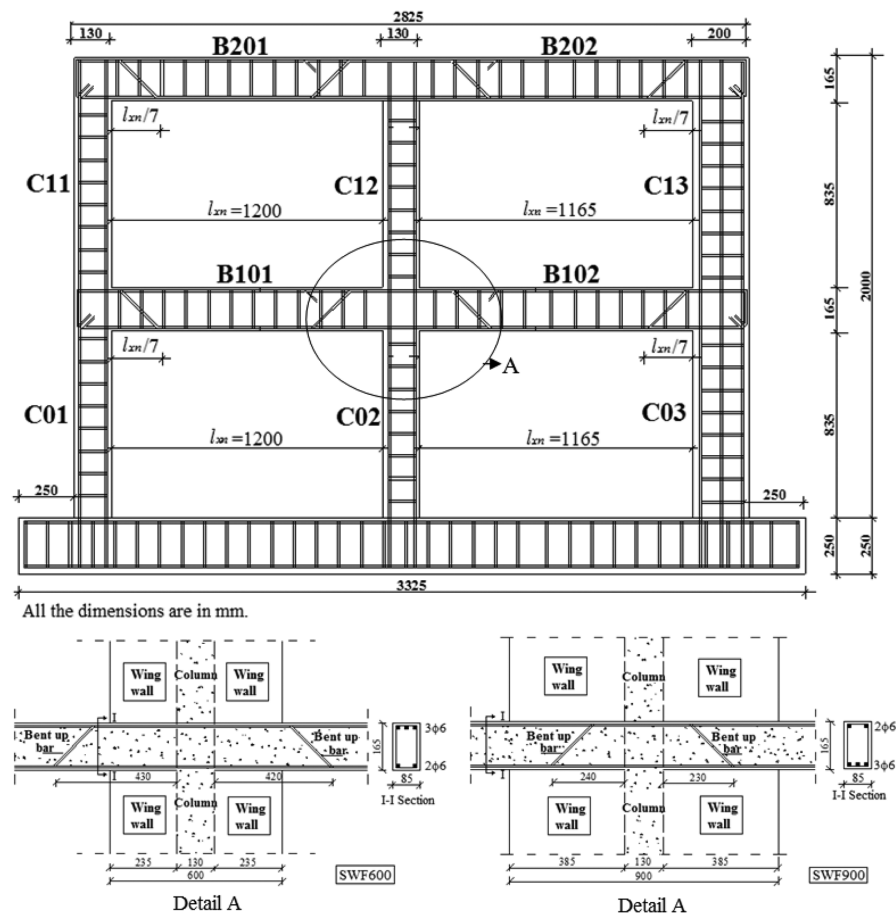
Fig. 2 Dimensions and reinforcement details of unstrengthened frames

Table 2 The dimensions and reinforcement layouts of columns and beams

	Columns		Beams		
Specimen	Left external and middle column (C01,C02,C11,C12)	Right external column (C03,C13)	Initial support region	New support region after strengthening	Midspan region
BF	4φ8 85 mm 130 mm	6φ8 85 mm 200 mm	3φ6 2φ6 165 mm 85 mm	3φ6 2φ6 165 mm 85 mm	2φ6 3φ6 165 mm 85 mm
SWF600	4φ8 85 mm 130 mm	6φ8 85 mm 200 mm	3φ6 2φ6 165 mm 85 mm	3φ6 2φ6 165 mm 85 mm	2φ6 3φ6 165 mm 85 mm
SWF900	4φ8 85 mm 130 mm	6φ8 85 mm 200 mm	3φ6 2φ6 165 mm 85 mm	2φ6 3φ6 165 mm 85 mm	2φ6 3φ6 165 mm 85 mm

All stirrups for using columns and beams were selected diameter of 4 mm and spaced 100 mm. Hook lengths of stirrups were applied 10φ. In here φ is bar diameter.
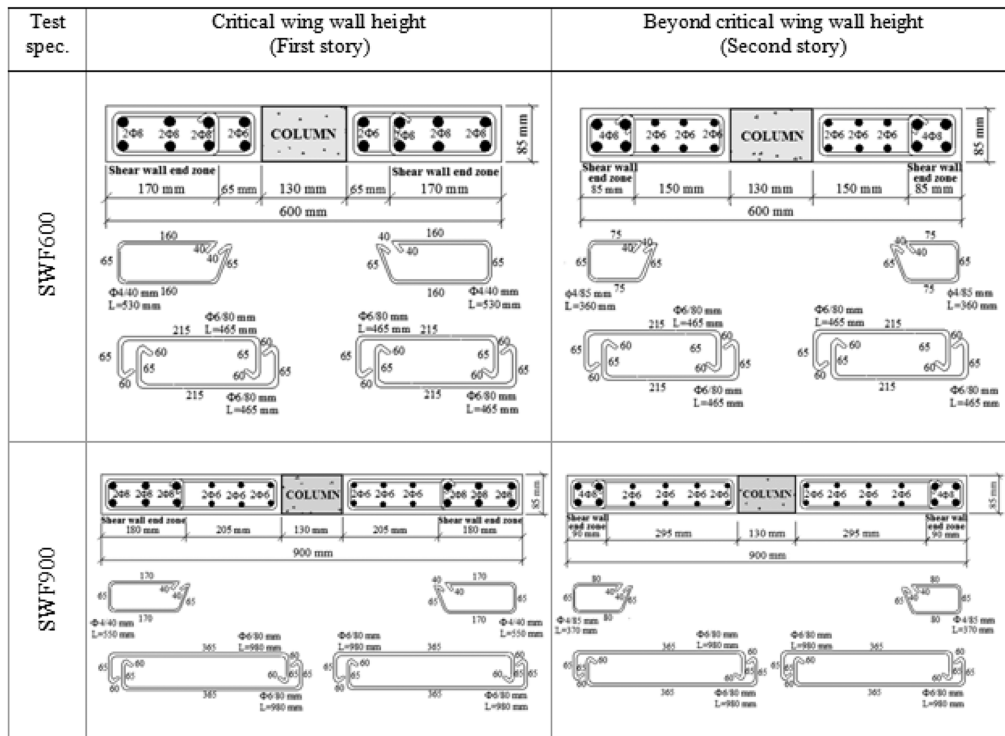

Fig. 3 Reinforcement layouts and dimensions of wing walls

SWF600   SWF900
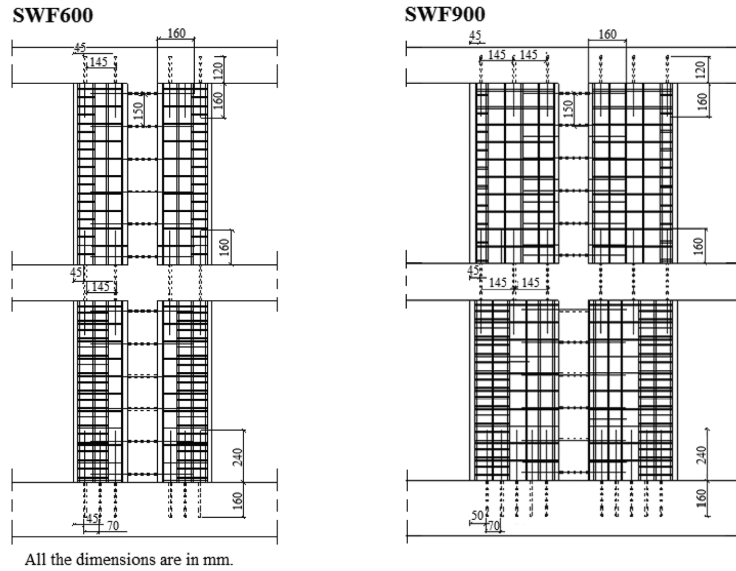

All the dimensions are in mm.

Fig. 4 Dowel spacing and embedment lengths of anchorage bars

which were placed in the holes and fixed by epoxy injection. Anchorage members were selected with a diameter of 8 mm for deformed bars, and holes were drilled with a diameter of 10 mm. The spacing of dowels was 150 mm, 145 mm and 70 mm for columns, beams and foundation levels, respectively. The embedment lengths of the anchorage bars into the wing walls were 160 mm (20ϕ) for beams and columns and 240 mm (30ϕ) for foundation levels. Each dowel consisted of one deformed bar centered at the face of the frame members. The frame specimens were cast in a horizontal position and tested in a vertical position. First, unstrengthened bare frames were produced and cured for 28 days under natural weather conditions. Then, in two frames, the dowels were drilled and anchored to the bare frames. After that step, the molds of the wing walls were placed on the frames with dowels, and the reinforcements of the wing walls were placed. Finally, the concrete in the walls was cast in situ horizontally. After the curing period of the wing walls was completed, the specimens were lifted to vertical using a special arrangement consisting of steel profiles surrounding the frame. This arrangement fixed the foundation of the specimen using transmission bolts.

Prior to casting the wing walls, rough surfaces were produced at the frame-wing wall interface to promote better bonding for all of the faces. The height and thickness of the reinforced concrete wing walls in all of the specimens were H_w: 2000 mm and b_w: 85 mm, respectively. The total length of the shear walls were chosen as 600 mm and 900 mm, and the strengthened frames with these walls were called SWF600 and SWF900, respectively. Therefore, two different aspect ratios of the shear walls involving the flexural and shear effects were used. A bare frame (BF) was designed to be the reference specimen. In all of the strengthened specimens, the frames were produced first, and the strengthening process was applied thereafter.

The concrete strength of the test frames and infill walls on the 28th day was 14.24 MPa and 30.24 MPa, respectively. The properties of the reinforcement material used in this study are listed in Table 3.

Table 3 Yielding and ultimate strength values of reinforcements

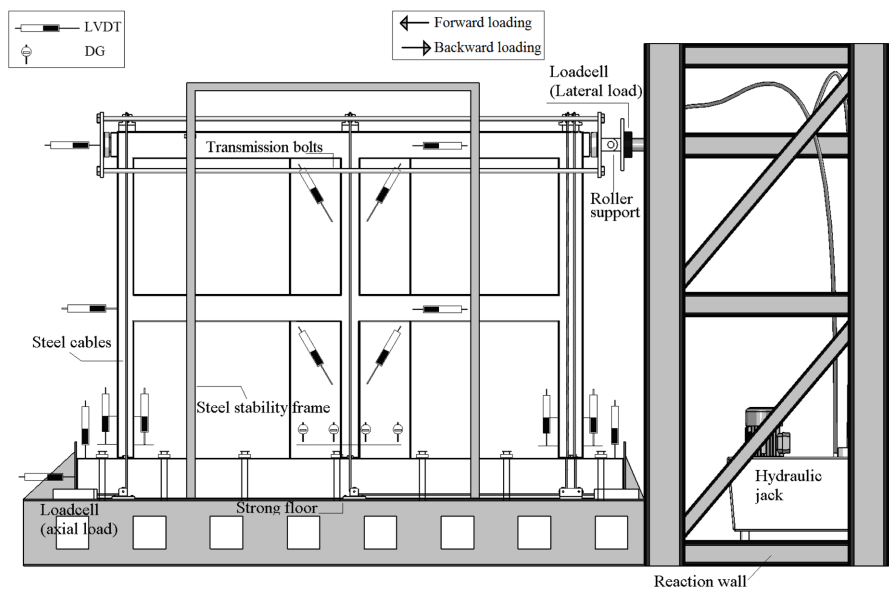| Bar diameter, mm	f_{sy} (MPa)	f_{su} (MPa)	Type
$\phi 4$	333	469	Plain
$\phi 6$	541	638	Plain
$\phi 8$	447	653	Plain
$\Phi 6$	529	664	Deformed
$\Phi 8$	525	766	Deformed

Fig. 5 Test set-up and instrumentation

2.2 Test set-up and instrumentation

The concrete in test specimens was cast in situ, and all of the cylindrical concrete samples were kept at air temperature for 28 days. The testing system consisted of the strong floor, the reaction wall, loading equipment, instrumentation, and a data acquisition system (Fig. 5). The foundations of the test specimens were fixed to the strong floor by high-strength steel bolts. The specimens were tested under a reversed cyclic lateral load that simulated the effects of an earthquake. A lateral load was applied to the top-story floor level using a hydraulic jack, and this load was transmitted to the frames using special countershafts. A steel stability frame was constructed around the test specimens to prevent out-of-plane movements. The lateral load value was measured by a bidirectional (compression-tension) load cell with a capacity of 500 kN. The lateral loading program was applied in a load-controlled manner until the yield stage, and it was subsequently applied in a displacement controlled manner in the following cycles until the end of the test.

The axial load was measured by one directional load cell with a capacity of 200 kN and was controlled continuously. The axial load was applied to each column using steel wire ropes placed in

a bobbin system prior to the application of the lateral load (approximately $0.10A_c f_c$ according to TBC500-2000). These limit values were determined according to the largest column cross-section for each test frame. The lateral displacements of the test specimens at each floor level were measured by displacement transducers (LVDT).

3. Test results

3.1 General observations and failure patterns

The nonstrengthened bare frame (BF) test provided reference data to allow for comparison with the performance of the wing wall-strengthened frames. The first crack in the nonstrengthened frame was detected in the right support of the first-story beam B102 at a load level of 15 kN during the 3rd forward cycle. The first cracking in the column was observed as a microcrack in the lower end of middle column at a load level of 20 kN during the 4th forward cycle. The maximum lateral load was 47.61 kN in the bare frame. At this load level, the top (upper story) lateral displacement of the frame was 51.60 mm. A 45° crack was observed in the upper end of the right exterior column (Fig. 6).
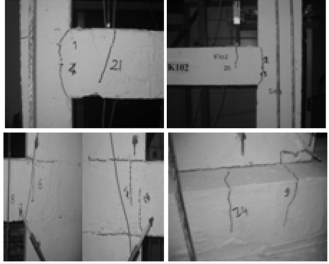
Fig. 6 Failure patterns of test specimens

SWF600   SWF900

Fig. 7 Damage to the shear wall-beam connections

The first crack in the SWF600 test specimen was detected in the right end of the first-story right beam (B102) at a load level of 20 kN during the 4th forward cycle. In the 11th forward cycle, at a load level of 60 kN, a 5th crack was observed at 200 mm from the right support of the B101 beam (bent bar breaking point). The first hairline crack in the base of the shear wall was 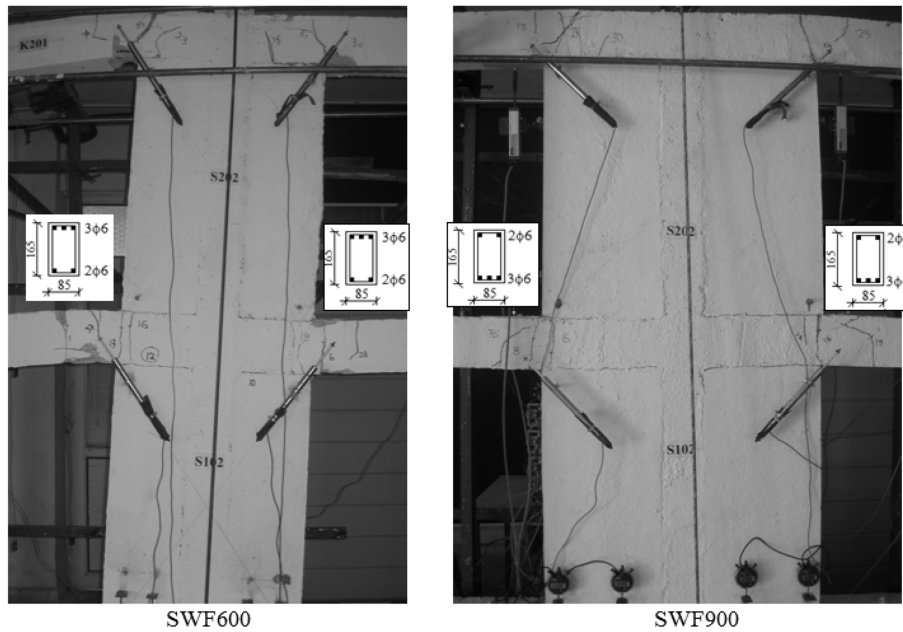observed at a load level of 80 kN during the 13th forward cycle. The width and length of the crack were measured as 0.02 mm and 400 mm (from the right end of the wall), respectively. In the 14th backward cycle, at a load level of 90 kN, a vertical crack occurred at the beam in the shear wall at $h_{beam}/4$ (one quarter of the beam height) away from the wall side. In the 15th forward cycle, at a load level of 100 kN, hairline cracks were observed on the right bottom end of the C01 column. In this phase, the top displacement was measured as 9.05 mm. The maximum lateral load was determined to be 116.67 kN. After this stage, sliding was shown at the shear wall-foundation connection, and the damage increased rapidly. No significant damage was observed in the side columns as a result of the energy dissipation at the shear wall (Fig. 6). Vertical cracks were observed in the beams in an area extending from the internal surface of the support to a length equal to the beam's height (disturbed (D) regions, Fig. 7). In this experiment, shear cracks at an angle of 45° developed on the beam-column connection (joint) because of the lack of a stirrup (Fig. 8).

The first crack in the SWF900 test specimen was detected on the left end of the first-story beam B101 at a load level of 30 kN during the 3th forward cycle. The first hairline crack on the shear wall-foundation connection occurred at a load level of 91.27 kN during the 7th forward cycle. In this phase, the lateral top displacement was measured as 2.94 mm. During the 7th backward cycle at a load level of 90 kN, vertical cracking developed in the shear wall at $h_{beam}/4$ from the side of the wall. The shear wall slid fully from the foundation during the 9th forward cycle at a load level of 130 kN and a top displacement of 5.9 mm. The first hairline cracks on the bases of the side
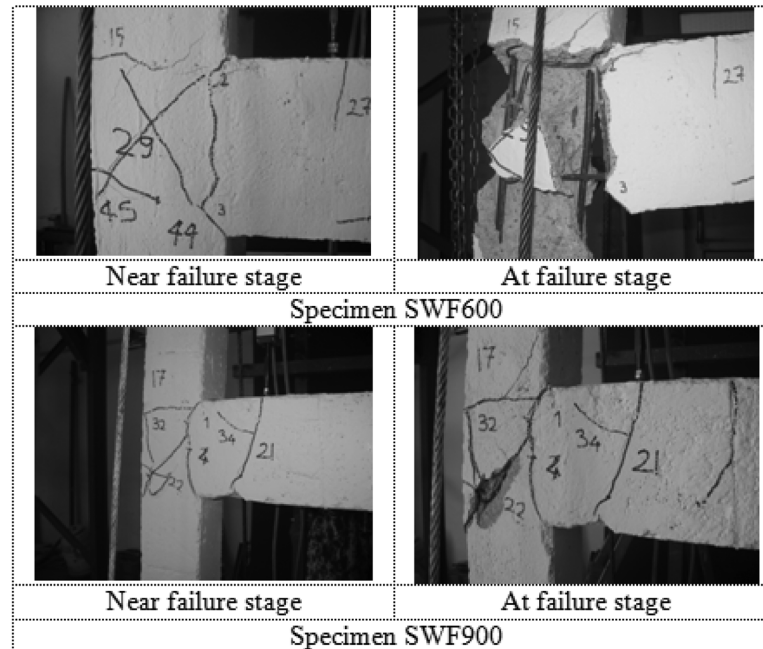
Fig. 8 Diagonal cracks from the left column to the beam joint

columns were observed at a lateral load level of 150 kN during the 10th backward cycle. The maximum lateral load was 174.64 kN for this frame. The lateral top displacement during this phase was 15.81 mm. After this phase, sliding appeared at the connection of the shear wall-foundation, and no important damage was observed in the frame members and the side columns as a result of energy dissipation by the shear wall (Fig. 6).

A general examination of the behavior of the nonstrengthened frame (BF) showed that there was hinge formation in the beam ends and column bases during the collapse phase, and vertical cracks were detected, particularly in all of the bent bar breaking zones of the first-story beams. In addition, a shear crack (at a 45° angle toward the horizontal surface) was detected on the side column, which was 200 mm in width (C03). A general evaluation of the behavior of the frames strengthened with wing walls showed that there were vertical cracks on the bent bar breaking zones of the beams and hinge formations on the beam ends and wall bases. The SWF600 test specimen showed vertical cracks in the shear wall section at a ($h_{beam}/4$) distance from the outer edge of the shear wall, and a shear crack (with an approximate angle of 45°) was detected on the left side of the beam-column connection (C01-B101) because there was no stirrup in the column. Concrete crushing and catastrophic failure occurred in the left exterior first story beam-column joint in test specimen SWF600 during the last cycle. In test specimen SWF900, no concrete crushing occurred, and only the width of previously formed cracks developed in this region. Vertical cracks were observed at the beam support regions with a length approximately equal to the beam height. However, no significant damage was recorded in the side columns of both strengthened frames. Significant damage was recorded in the beam ends of the SWF600 test specimen. Generally, no significant damage was observed in the test specimen SWF900. The experimental observations indicate that the wing walls moved monolithically with the central column of the frame; the maximum lateral load

capacity of specimen SWF900 increased by 50% compared with test specimen SWF600, and the level of damage to the SWF900 frame was significantly reduced because of the 50% increase in the total length of the shear wall. The general behaviors of tested specimens are presented in Fig. 6 at maximum lateral load and failure load levels. In addition, the beam-column joint damage to the strengthened frames is shown in Fig. 8.

4. Discussion of test results

4.1 Strength and displacement ductility

"Lateral load-top displacement" hysteresis curves of the test specimens are shown in Fig. 9. Lateral load-top displacement curves are used to observe the strength and stiffness values of a test specimen and to evaluate the general behavior of a frame. For lateral load-top displacement curves, the maximum lateral load-bearing capacities of the BF, SWF600 and SWF900 test specimens were 47.61, 116.67 and 174.64 kN, respectively. Using the reference frame (BF) as the baseline, the maximum increase in the load-bearing capacity was determine to be 145% for the system with a 600 mm shear wall (SWF600) and 267% for the system with a 900 mm shear wall (SWF900). The maximum displacements corresponding to a 20% decrease in lateral load capacity were measured as approximately 100, 40 and 25 mm for the BF, SWF600 and SWF900 test specimens, respectively.

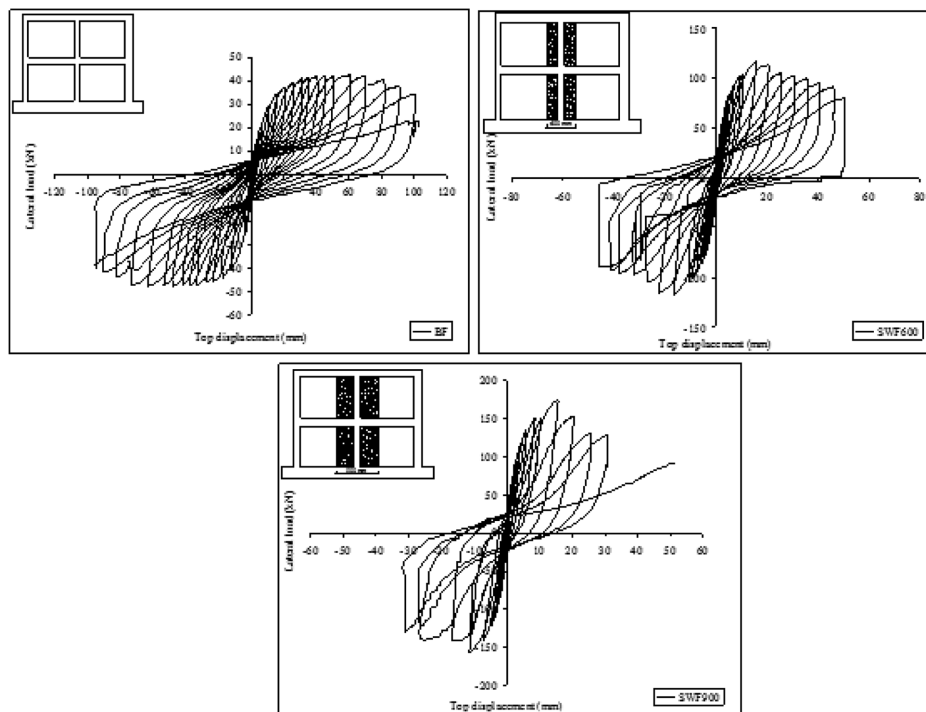A lower displacement measurement was recorded in the SWF600 compared with the reference

Fig. 9 Hysteresis curves of the test specimens

Table 4 Lateral load and top story displacement values of test specimens

Loading direction	Specimen	Yielding		Maximum lateral load		Failure load*		Disp. ductility ratio
		Load (kN)	Top displ. (mm)	Load (kN)	Top displ. (mm)	Load (kN)	Top displ. (mm)	
Forward	BF	31.45	13.01	41.93	38.12	33.54	96.42	7.41
	SWF600	88.8	6.91	116.67	15.63	93.34	43.58	6.31
	SWF900	134.68	6.80	174.64	15.81	139.71	25.51	4.58
Backward	BF	35.71	11.72	47.61	51.60	38.09	94.16	8.03
	SWF600	90.77	7.33	116.43	12.13	93.14	41.14	5.61
	SWF900	123.83	5.30	156.88	6.40	125.50	31.00	5.85

bare frame; however, significant damage to the frame system was not prevented. The maximum lateral load capacity of SWF900 was 50% greater than SWF600. In addition, frame damage was significantly reduced, and no significant damage was observed in the columns. This shows that it is better to use shear walls of sufficient stiffness (sufficient length). In such cases, system strengthening may be more successful, and the need to strengthen other frame members may be eliminated.

The tests were performed on undamaged, vulnerable RC frames. The most important outcome of these tests is that no important damage occurred on the side columns under weak earthquake activity until the load-bearing capacity of the shear wall was exceeded, which proves that shear walls are effective for lateral load bearing. The main damage accumulated at the ends of beams connected to the shear wall. The vertical cracks on the beams occurred in strengthened specimens. The cracks formed because of the insufficient capacity of beams under changing directions of moments, due to the effect of reversed cyclic loads. The positive moment capacities of beams at the support region (connection of the beam-shear wall) were 4378 kN mm for SWF600 and 6429 kN mm for SWF900. Less damage to beam-shear wall connections was observed in the SWF900 specimen compared with the SWF600 specimen because of the decrease of the ultimate displacement (Fig. 7).

The test results were compared in terms of lateral load capacity, stiffness and displacement ductility ratio. Table 4 shows yielding, the maximum and failure loads and the corresponding displacement values. The yielding displacement was calculated on the basis of a bilinear approximation of the lateral load-top displacement envelope curve. The δ_{80} displacement value is the ultimate displacement corresponding to a 20% decrease in the lateral load capacity (Kazemi and Morshed 2005). This value was assumed to represent the failure displacement of the frames. The displacement ductility ratios of the test frames were determined using the lateral load-top displacement curves according to this value. These values were computed as the ratio of the failure load displacement to the yielding load displacement (Table 4). The highest displacement ductility ratio was obtained for the unstrengthened bare frame.

4.2 Stiffness

The initial (tangent) stiffness and collapse stiffness values of the test specimens are listed in Table 5. Tangent stiffness is defined as the initial slope of the lateral load-top displacement curve. Collapse

Table 5 Stiffness values of test specimens

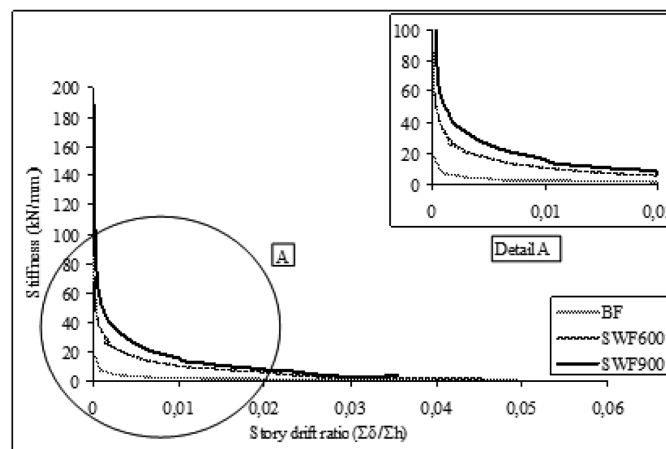| Specimen No	Initial, R_i (kN/mm)	Collapse R_c, (kN/mm)	R_i/R_{ref}	R_c/R_{ref}	Stiffness Degredation, %	R/R_{ref}
BF*	17.11	0.41	-	-	97.60	-
SWF600	84.70	2.91	4.95	7.10	96.56	0.99
SWF900	188.06	8.14	10.99	19.85	95.67	0.98

*Reference specimen

Fig. 10 Comparison of the stiffness degradation curves

stiffness is defined as the mean of the slope of the lines connecting the origin with the peak points of the collapse load. This stiffness value was determined using the ultimate displacement corresponding to a 20% decrease in the lateral load capacity. The initial stiffness of the BF, SWF600 and SWF900 specimens was calculated as 17.11, 84.70 and 188.06 kN/mm, respectively. The stiffness decreased during subsequent cycles (Fig. 10). An evaluation of the stiffness values on the basis of the reference test frame (BF) showed that the initial stiffness value of the SWF600 specimen increased 4.95-fold, and the SWF900 specimen increased 10.99-fold. The collapse stiffness value of the SWF600 specimen increased 7.10-fold, and the SWF900 specimen increased 19.85-fold. For both stiffness types, the SWF900 test specimen generated the highest stiffness values, and the BF specimen generated the lowest values. Accordingly, the bare frame (BF) produced the highest (97.60%) and SWF900 the lowest (95.67%) stiffness decrease in the collapse phase. For all of the test frames, the stiffness degradation values were determined to be similar.

4.3 Energy dissipation

The energy dissipation characteristic of the structural members plays an important role in the behavior of structures against earthquake effects. Members with perfect plastic behavior dissipate some energy during each cycle of loading. For each test specimen, the energy dissipated in each cycle was obtained by calculating the area enclosed by the corresponding lateral load-top

displacement hysteretic loop. The dissipated cumulative energy was subsequently calculated by summing the energy dissipated during consecutive cycles throughout the test. The limit for the energy dissipation comparison was determined to be the ultimate displacement corresponding to a 20% decrease in the lateral load capacity. Considering the limit value, the dissipated energy values were calculated as 19083.61, 22501.40 and 20362.10 kN mm for the BF, SWF600 and SWF900 test specimens, respectively. Considering the displacement at the maximum lateral load level, the dissipated energy values were 533.35, 3663.39 and 4839.84 kN mm for the BF, SWF600 and SWF900 test specimens, respectively. Considering the displacement at the end of the test, the dissipated energy values were 21271.80, 25100.73 and 30371.88 kN mm for the BF, SWF600 and SWF900 test specimens, respectively. When the energy absorption capacities of the strengthened frames at a failure load displacement (corresponding to 80% of the maximum lateral load) were compared, the SWF600 specimen showed a greater energy absorption value than SWF900. The damage level decreased for SWF900, which is desirable. The strengthened frame SWF900 was shown to be more rigid. When comparing the energy absorption capacities of the strengthened frames corresponding to the maximum load and at the end of the test, SWF900 showed the greatest energy absorption capacity.

5. Analytical results

An analytical investigation evaluated the capacity curve and the general behavior of each test specimen. A nonlinear static analysis (static pushover analysis) was used to determine the response envelope curves of frames beyond the elastic limit. The pushover analysis method has become a powerful method for seismic design (Makarios 2005, Inel and Ozmen 2006). After the computer model of the building is prepared for the nonlinear pushover analysis, the hinge properties of the components should be defined. The hinge properties specify the plastic rotation values that the end of a component can withstand and the acceptable plastic rotation values for the performance level. In ATC-40 and FEMA-356, the hinge properties are given according to the component type and failure mechanism. The SAP2000 software program was used for these processes.

Plastic hinges at the end of the beams and columns were placed at half of the height of the cross section. The vertical load level of the shear walls was notably low compared with the axial load-
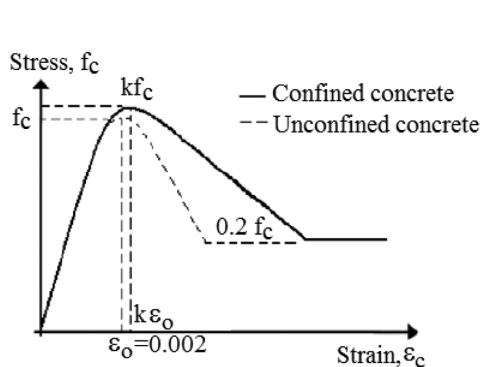

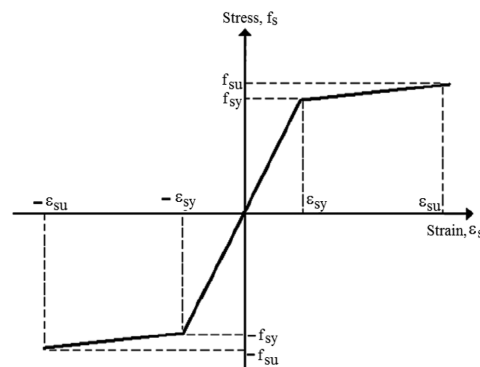Fig. 11 Stress-strain relation of the concrete (Arslan 2010)

Fig. 12 Stress-strain relation of the steel (Arslan 2010)
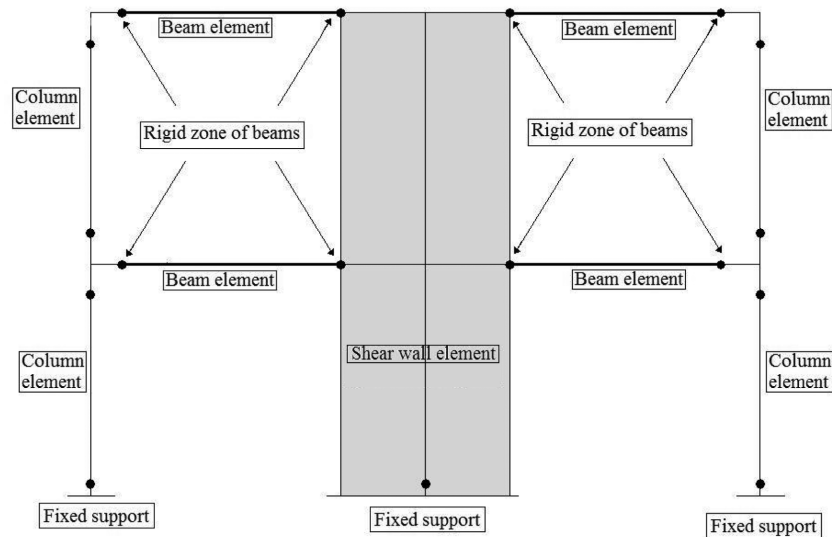
Fig. 13 Analytical model of specimens with shear walls
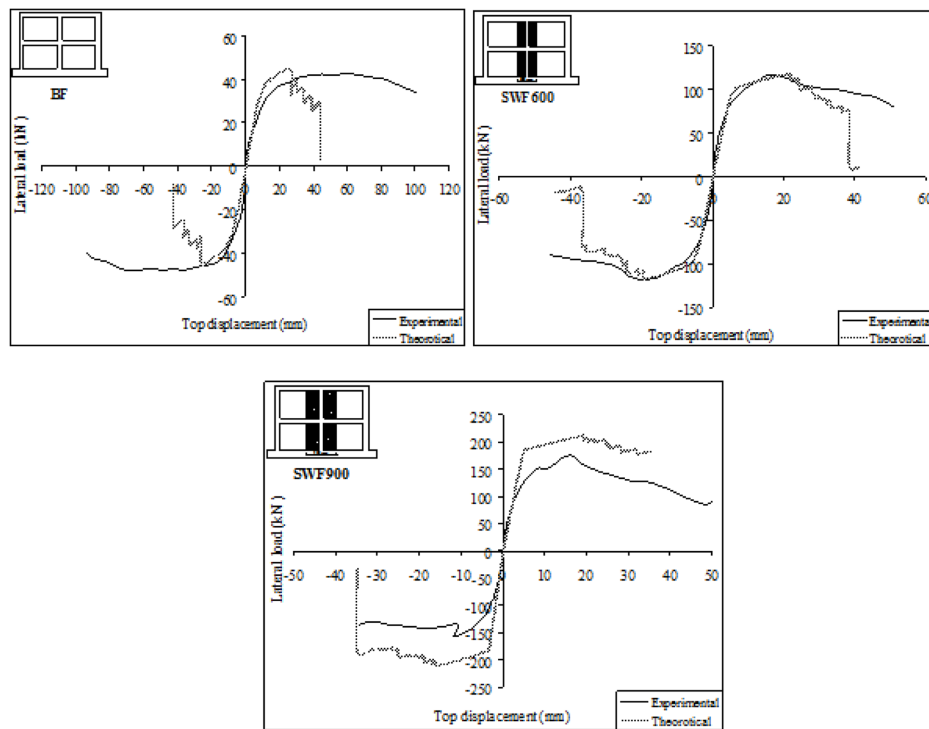

Fig. 14 Comparative lateral load-top displacement envelope curves of the test frames

bearing capacity (approximately 10% $A_c f_c$). Therefore, a likely bending (moment) hinge was assigned to the shear walls to represent the behavior of the RC section under the effect of a flexure.

In this study, the envelope curve introduced by Kent and Park (1971) and later extended by Scott

Table 6 Comparison of experimental and analytical results

Loading Direction	Specimen	Maximum Lateral Load, kN			Failure Displacement*, mm		
		Experimental	Analytical	Ratio	Experimental	Analytical	Ratio
Forward	BF	41.93	44.51	0.94	96.42	33.99	2.84
	SWF600	116.67	117.64	0.99	43.58	28.75	1.52
	SWF900	174.64	212.37	0.82	25.51	32.11	0.79
Backward	BF	47.61	44.75	1.06	94.16	33.45	2.81
	SWF600	116.43	116.71	1.00	41.14	25.83	1.59
	SWF900	156.88	210.64	0.74	31.00	26.48	1.17

*This failure displacement value was determined by using ultimate displacement corresponding to 20% decrease in lateral load capacity.

et al. 1982) was used. The stress-strain relationship in the proposed model given in Fig. 11 was developed for concrete that was confined by rectangular hoops. ε_{co} is the concrete strain at maximum stress, and k is a factor that accounts for the increase in strength caused by confinement. An idealized stress-strain relationship for a steel reinforcement is shown in Fig. 12. The reinforcement is modeled as a linear elastic, linear strain, hardening material under yield stress (Mander 1984). The behavior of the RC members is greatly affected by the yielding of steel when the section is subjected to monotonic bending moments (Arslan 2010).

A lateral load was applied to the axis of the top story beam and to one of the mass-concentrated sections. An analytical model for specimens with shear walls is given in Fig. 13. The beams of the frame were modeled as two pieces and were connected to the middle axis of the shear wall.

Fig. 14 compares the experimental and analytical response envelope curves of the tested frames.

Table 6 shows that the experimental and analytical maximum lateral load-bearing capacities are similar for BF (±6%) and SWF600 (+1%, −0%) specimens with analytical values. The greatest difference was recorded in the lateral load-bearing capacity of the SWF900 specimen (±26%). It is likely that different displacements also occurred. It is thought that these differences developed as a result of the sliding of the anchorage bars in the foundation such that the shear wall could not reach its full capacity. Another explanation for the difference is the occurrence of relatively slight damage to nodal zones, which were assumed to be rigid end zones during the experiment. Arslan *et al.* (2010) found the same differences in an analytical study that was performed for a two-story, two-bay RC frame.

6. Conclusions

This study consisted of an experimental and analytical analysis of the reversed cyclic lateral load behaviors of three units of multi-story, multi-bay, reinforced concrete frames (one bare and the remaining two strengthened with concrete wing walls), which had weak earthquake resistance and insufficient seismic detail. The basic parameters considered in the strengthened specimens were the total length of the shear wall and the location of the bent bar reinforcement (in the beam) that was integrated into the shear wall. These specimens had different total shear wall height/shear wall

length (H_w/L_w) ratios and were strengthened via the integration of a reinforced concrete wing wall on both sides of the central column. They were subjected to reversed cyclic lateral loads in a vertical position, simulating the effects of an earthquake to observe their seismic behaviors.

According to experimental observations:

* The wing walls and frame columns worked monolithically in both applications.

* In both strengthening frames, no serious damage was observed on the frame elements until reaching the maximum lateral load level.

* Based on the test results, it was concluded that the use of a reinforced concrete wing wall considerably increased the lateral load-bearing capacity, stiffness and energy dissipation capacity of the existing vulnerable frame system and that this type of shear wall strengthening successfully rehabilitates/improves the system. Furthermore, the transformation of a column to a shear wall of sufficient length and size may reduce or eliminate the need to strengthen other weak columns.

The specific results obtained from experimental and analytical studies can be summarized as follows:

* At the end of the experiments, SWF600 showed a 178%-144% (forward-backward cycle, respectively) greater lateral load bearing capacity, and SWF900 displayed a 316%-229% (forward-backward cycle, respectively) greater lateral load bearing capacity. SWF900 showed a 49%-34% (forward-backward cycle, respectively) greater lateral load bearing capacity than the SWF600 specimen. The maximum displacements corresponding to a 20% decrease in the lateral load capacity were measured as approximately 100, 40 and 25 mm for the BF, SWF600 and SWF900 test specimens, respectively. It is obvious that the failure load displacement is limited by increasing the shear wall's length.

* The SWF900 test specimen generated the highest stiffness values, and the BF specimen generated the lowest values for the initial and collapse stiffness. An evaluation of the stiffness values between the two strengthened frames showed that the initial and collapse stiffness value of the SWF900 specimen increased 2.22 times and 2.79 times, respectively, compared with the SWF600 specimen.

* Bending cracks were observed on the first-story beams of the strengthened frames because of the insufficient moment capacity of beams under changing directions of moment, due to the effect of reversed cyclic loads. Furthermore, less damage to the beam-shear wall connections was observed in SWF900 specimen than in the SWF600 specimen because of the decrease of the ultimate displacement.

* Vertical cracks were observed in the shear wall-beam connections at a distance nearly equal to the beam height because of the stress concentration caused by the support for the strengthened frames. Because the beams between the shear wall and the side column became coupling beams in the strengthened frames, significant damage and hinge formation were observed at the ends of these elements.

* The changing of the aspect ratio of the shear wall did not affect the general cracking behavior of the strengthened frames and the failure mechanism. No shear failure occurred in the strengthened frame with a large aspect ratio (SWF900). Bending cracks occurred in both strengthened frames because of the low vertical load level. The bent bars of the beams in the SWF600 specimen came out of the wing wall section, and vertical bending cracks were observed in this region. The bent bars of the beams in the SWF600 specimen remained in the wing wall section, and any damage occurring at this point on the beam because of the wing walls moved monolithically with the central column of the frame as a shear wall.

* The wing wall-foundation anchorage rods slid in the connection zone in the SWF900 test specimen. It is believed that the reason for this result was the insufficient number and length of anchorage bars and that the foundation had poor concrete compression strength.

* When the energy absorption capacities of the strengthened frames at a failure load level were compared, the SWF600 specimen showed a higher energy absorption value than SWF900 did. However, the damage level decreased in SWF900, which is desirable. For the energy absorption capacities of the strengthened frames corresponding to a maximum load and at the end of the test, the greatest energy absorption capacity was shown for SWF900.

* In the analytical part of this study, a pushover analysis was performed using the SAP2000 program. The experimental and theoretical maximum lateral load-bearing capacities were found to be very similar for the BF and SWF600 specimens. The greatest difference was recorded in the lateral load-bearing capacity of the SWF900 specimen as a result of the sliding of the anchorage bars in the foundation. The experimental and analytical maximum lateral load-bearing capacities were very similar between the BF ($\pm6\%$) and SWF600 ($+1\%$, -0%) specimens and the analytical values. The greatest difference was recorded for the lateral load-bearing capacity of the SWF900 specimen ($\pm26\%$). The reasons for this difference were the sliding of the anchorage bars in the foundation and the development of damage at nodal zones that were assumed to be rigid end zones during the experiment.

Reinforced concrete wing walls can be used for structural system strengthening in cases in which shear walls cannot be constructed using the "complete filling of frame spans" technique because of architectural reasons or other concerns. One of the most important components of the strengthening procedure is to ensure that a perfect bond exists between the existing structural system and the new members. In earthquake-prone countries and regions where most of the building stock is composed of RC buildings with poor earthquake tolerance, these buildings should be promptly strengthened, considering their conditions of use, their importance and the architecture of the buildings to prevent further damage and destruction in the event of an earthquake.

Acknowledgements

References

Anil, Ö. and Altin, S. (2007), "An experimental study on reinforced concrete partially infilled frames", *Eng. Struct.*, **29**(3), 449-460.

Aoyama, H., Kato, D., Katsumata, H. and Hosokawa, Y. (1984), "Strength and behavior of postcast shear walls for strengthening of existing R/C buildings", *Proceedings of the 8th World Conference on Earthquake Engineering,* San Francisco, July.

Arslan, M.H. (2010), "An evaluation of effective design parameters on earthquake performance of RC buildings using neural networks", *Eng. Struct.*, **32**, 1888-1898.

Arslan, M.H., Yüksel, I. and Kaltakcı, M.Y. (2010), "An investigation on global ductility of strengthened RC frames", *Proceedings of the Institution of Civil Engineers-Structures and Buildings*, **163**(3), 177-194.

ATC-40, FEMA Reports "Seismic evaluation and retrofit of concrete buildings", Applied Technology Council, November 1996, Vol. I ve II, Redwood City, California, USA.

Canbay, E., Ersoy, U. and Ozcebe, G. (2003), "Contribution of reinforced concrete infills to seismic behavior of structural systems", *ACI Struct. J.*, **100**(5), 637-643.

FEMA 273/356, Federal Emergency Management Agency, Guidelines for the seismic rehabilitation of buildings, Cilt I, Redwood City, California, USA.

Frosch, R.J., Li, W., Jirsa, J.O. and Kreger, M.E. (1996), "Retrofit on non-ductile moment-resisting frames using precast infill wall panels", *Earthq. Spectra*, **12**(4), 741-760.

Frosch, R.J. (1999), "Panel connections for precast concrete infill walls", *ACI Struct. J.*, **96**(4), 467-472.

Fukuyama, H. and Sugano, S. (2000), "Japanese seismic rehabilitation of concrete buildings after the Hyogoken-nanbu earthquake", *Cement Concrete Compos.*, **22**, 59-79.

Higashi, Y., Endo, T. and Shimizu, Y. (1984), "Experimental studies on retrofitting of reinforced concrete building frames", *Proceedings of the 8th World Conference on Earthquake Engineering*, San Francisco, July.

Inel, M. and Ozmen, H.B. (2006), "Effects of plastic hinge properties in nonlinear analysis of reinforced concrete buildings", *Eng. Struct.*, **28**(11), 1494-1502.

Jirsa, J.O. (2006), "Learning from earthquakes to improve rehabilitation guidelines for reinforced concrete buildings", *Adv. Earthq. Eng. Urban Risk Reduct. Nato Science Series: IV: Earth and Environmental Sciences*, **66**, 209-227.

Kahn, L.F. and Hanson, R. (1979), "Infilled walls for earthquake strengthening", *J. Struct. Div.*, **5**, 283-296.

Kara, M.E. and Altin, S. (2006), "Behavior of reinforced concrete frames with reinforced concrete partial infills", *ACI Struct. J.*, **103**(5), 701-709.

Kazemi, M.T. and Morshed, R. (2005), "Seismic shear strengthening of R/C columns with ferrocement jacket", *Cement Concrete Compos.*, **27**(7-8), 834-842.

Kent, D.C. and Park, R. (1971), "Flexural members confined concrete", *J. Struct. Div.*, **97**, 1969-1989.

Makarios, T.K. (2005), "Optimum definition of equivalent non-linear SDF system in pushover procedure of multistory RC frames", *Eng. Struct.*, **27**(5), 814-825.

Mander, J.B. (1984), "Seismic design of bridge piers", Research Report 84-2. Christchurch (New Zealand): Department of Civil Engineering, University of Canterbury.

Pincheira, J.A. and Jirsa, J.O. (1995), "Seismic response of RC frames retrofitted with steel braces or walls", *J. Struct. Eng.-ASCE,* **121**(8), 1225-1235.

SAP2000 V-7.4. "Integrated finite element analysis and design of structures basic analysis reference manual", Computers and Structures Inc., Berkeley, CA.

Scott, B.D., Park, R. and Priestley, M.J.N. (1982), "Stress_strain behavior of concrete confined by overlapping hoops at low and high strain rates", *ACI J.*, **79**(1), 13-27.

Sonuvar, M.O., Ozcebe, G. and Ersoy, U. (2004), "Rehabilitation of reinforced concrete frames with reinforced concrete infills", *ACI Struct. J.*, **101**(4), 494-500.

Sugano, S. and Fujimura, M. (1980), "Aseismic strengthening of existing reinforced concrete buildings", *Proceeding of the 7th World Conference on Earthquake Engineering*, Istanbul, Turkey.

Sugano, S. (2006), "Recent advances in the seismic rehabilitation of reinforced concrete buildings in Japan", *Adv. Earthq. En. Urban Risk Reduct. Nato Science Series: IV: Earth and Environmental Sciences*, **66**, 19-31.

TBC-500-2000, Turkish Building Code (2000), "Requirements for design and construction of reinforced concrete structures", Turkish Standards Institute, Ankara, Turkey.

TEC-1998, Turkish Earthquake Code (1998), "Specification for structures to be built in disaster areas", Ministry of Public Works and Settlement, Ankara, Turkey.

TEC-2007, Turkish Earthquake Code (2007), "Specifications for structures to be built in seismic areas", Ministry of Public Works and Settlement, Ankara, Turkey.

Yamamoto, Y. (1993), "Strength and ductility of frames strengthened with steel bracing", Earthquake Resistance of Reinforced Concrete Structures, A Volume Honoring Hiroyuki Aoyama, **25**, 467-476.

Yavuz, G. (2005), "The seismic behaviour of non-ductile reinforced concrete frames having poor seismic performance with partially reinforced concrete shear walls", PhD Thesis, Selcuk University, Konya, Turkey.

Yuce, S.Z., Yuksel, E., Bingol, Y., Taksin, K. and Karadogan, H.F. (2007), "Local thin jacketing for the retrofitting of reinforced concrete columns", *Struct. Eng. Mech.*, **27**(5), 589-607.

Notations

A_c	: Cross-sectional area of concrete
BF	: Unstrengthened frame
f_c	: Concrete compressive strength
f_{su}	: Ultimate strength of reinforcement bar
f_{sy}	: Yielding strength of reinforcement bar
H_w	: Total shear wall height
L_w	: Total shear wall length
LVDT	: Linear variable displacement transducer
P_{80}	: 80% of measured maximum lateral load
R	: Structural behavior factor
R_i	: Initial stiffness
R_c	: Collapse stiffness
SW	: Shear wall
δ_{80}	: Displacement value corresponding to 80% of the measured maximum lateral load
ϕ	: Diameter of plain reinforcement bar
Φ	: Diameter of deformed reinforcement bar